Inorganic Chemistry
Article

Inorg. Chem. **2011**, *50*, 231–237 **231**
DOI: 10.1021/ic101841a

Changes in Electronic Properties of Polymeric One-Dimensional $\{[M(CN)_2]^-\}_n$ (M = Au, Ag) Chains Due to Neighboring Closed-Shell Zn(II) or Open-Shell Cu(II) Ions

François Baril-Robert,[†] Xiaobo Li,[†] Michael J. Katz,[‡] Andrew R. Geisheimer,[‡] Daniel B. Leznoff,[‡] and Howard Patterson*,[†]

[†]*Department of Chemistry, University of Maine, Orono, Maine 04473, United States, and*
[‡]*Department of Chemistry, Simon Fraser University, Burnaby, British Columbia V5A 1S6, Canada*

Received September 7, 2010

A series of d^{10} dicyanometallate polymeric compounds were studied by electronic spectroscopy and density functional theory (DFT) calculations. In these materials, the negatively charged one-dimensional (1D) polymeric chains are linked together by $[M(en)_2]^{2+}$ (M = Cu(II) and Zn(II); en = ethylenediamine). More than innocent building blocks, the $[M(en)_2]^{2+}$ units offer a possible synthetic way to modify electronic properties of the materials. Through its low energy d-d excited state, the d^9 copper(II) ions offer deactivation pathways for the normally emissive dicyanometallate polymer. Deactivation was shown to be specific to the excited state energy.

Introduction

Intermolecular interactions are often harnessed to synthesize crystals with desirable topologies and structures.[1−6] In organic chemistry, hydrogen-bonding and $\pi-\pi$ interactions are often used to increase dimensionality and to promote the formation of materials with interesting three-dimensional (3D) structures.[7−9] The resulting compounds may exhibit porous structures which could potentially exhibit zeolitic properties. The crystal engineering toolbox can be increased by using metal ions,[10−14] which introduce the ability to form coordinate bonds and metallophilic interactions. In this regard, the dicyanoaurate(I) and −argentate(I) anions efficiently combine these two structural features: the dicyanometallate anions interact with neighboring metal cations[15] via bridging N-cyano coordinate bonds and with other $[M(CN)_2]^-$ units via metallophilic interactions (∼5−15 kcal/mol).[16] Moreover, these linear dicyanometallates often show luminescent behavior; thus, photophysical studies of $[M(CN)_2]^-$ based materials can be used to probe the interactions present and understand their electronic structure.[17,18] For example, in $K_2Na[Ag(CN)_2]_3$ and dicyanoargentate ions doped in alkali halides, a read/write/erase phenomenon has been reported.[19,20] In another study, the spectroscopic properties of two-dimensional (2D) polymeric networks of dicyanoaurate compounds in their alkali salts were carefully studied, and a clear direct relationship between energy and Au−Au distances was shown. Recently, Patterson and co-workers reported for the first time on a new heterobimetallic system, $Tb[Ag_xAu_{1-x}(CN)_2]_3$. In this case, energy transfer occurs from the tunable $[Ag_xAu_{1-x}(CN)_2]^-$ donor ions to the luminescent Tb^{3+} acceptor ions with the energy tunability of the donor ions dependent on the Ag/Au stoichiometric ratio.[21−23]

*To whom correspondence should be addressed. E-mail: howardp@maine.edu.

(1) Moulton, B.; Zaworotko, M. J. *Chem. Rev.* **2001**, *101*, 1629–1658.
(2) Northrop, B. H.; Zheng, Y. R.; Chi, K. W.; Stang, P. J. *Acc. Chem. Res.* **2009**, *42*, 1554–1563.
(3) Davis, T.; Spada, G. P. *Chem. Soc. Rev.* **2007**, *36*, 296–313.
(4) Steed, J. W.; Atwood, J. L. *Supramolecular Chemistry*, 2nd ed.; John Wiley & Sons: Sussex, U.K., 2009.
(5) Brammer, L. *Chem. Soc. Rev.* **2004**, *33*, 476–489.
(6) Hollingsworth, M. D. *Science* **2002**, *295*, 2410–2413.
(7) Wuest, J. D. *Chem. Commun.* **2005**, 5830–5837.
(8) Reichenbächer, K.; Süss, H. I.; Hulliger, J. *Chem. Soc. Rev.* **2005**, *34*, 22–30.
(9) Desiraju, G. R. *Acc. Chem. Res.* **2002**, *35*, 565–573.
(10) Katz, M. J.; Sakai, K.; Leznoff, D. B. *Chem. Soc. Rev.* **2008**, *37*, 1884–1895.
(11) Blake, A. J.; Champness, N. R.; Hubberstey, P.; Li, W.; Withersby, M. A.; Schröder, M. *Coord. Chem. Rev.* **1999**, *183*, 117–138.
(12) Batten, S. R.; Neville, S. M.; Turner, D. R. *Coordination Polymers: Design, Analysis and Application*; RSC Publishing: Cambridge, 2008.
(13) Phan, A.; Doonan, C. J.; Uribe-Romo, F. J.; Knobler, C. B.; O'Keeffe, M.; Yaghi, O. M. *Acc. Chem. Res.* **2010**, *43*, 58–67.
(14) Shimomura, S.; Bureekaew, S.; Kitagawa, S. *Struct. Bonding (Berlin)* **2009**, *132*, 51–86.
(15) Triščíková, L.; Potočňák, I.; Chomič, J.; Baran, P. *Transition Met. Chem.* **2006**, *31*, 504–515.
(16) Schmidbaur, H.; Schier, A. *Chem. Soc. Rev.* **2008**, *37*, 1931–1951.
(17) Rawashdeh-Omary, M. A.; Omary, M. A.; Patterson, H. H. *J. Am. Chem. Soc.* **2000**, *122*, 10371–10380.
(18) Rawashdeh-Omary, M. A.; Omary, M. A.; Patterson, H. H.; Fackler, J. P., Jr. *J. Am. Chem. Soc.* **2001**, *123*, 11237–11247.
(19) Hettiarachchi, S. R.; Patterson, H. H.; Omary, M. A. *J. Phys. Chem B* **2003**, *107*, 14249–14254.
(20) Omary, M. A.; Colis, J. C. F.; Larochelle, C. L.; Patterson, H. H. *Inorg. Chem.* **2007**, 3798–3800.
(21) Lu, H.; Yson, R.; Ford, J.; Tracy, H. J.; Carrier, A. B.; Keller, A.; Mullin, J. L.; Poissan, M. J.; Sawan, S.; Patterson, H. H. *Chem. Phys. Lett.* **2007**, *443*, 55–60.
(22) Colis, J. C. F.; Staples, R.; Tripp, C.; Labrecque, D.; Patterson, H. H. *J. Phys. Chem. B* **2005**, *109*, 102–109.

Published on Web 12/08/2010

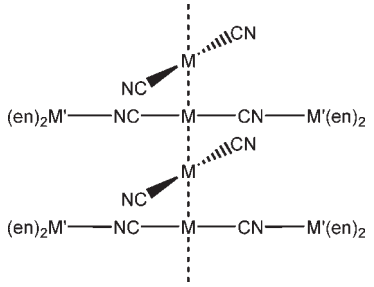

Figure 1. Metallophilic 1D polymeric structure of $[M'(en)_2][M(CN)_2]_2$ (where M = Ag, Au and M′ = Cu, Zn).

Using standard coordination polymer synthetic methodologies, by judiciously selecting a mixture of dicyanometallate building blocks, metal cations, and, when appropriate, polyamine ligands, a series of multidimensional coordination polymer materials can be obtained.[24−27] For example, a series of compounds with the general formula $[PbL_{1or2}][Au(CN)_2]_2$ (L = 1,10-phenanthroline; 2,2′-bipyridine, and ethylenediamine) show the effect of the ligand on the sp-hybridization of the lead metal center.[28] In the ethylenediamine-containing compounds, the short contact between gold(I) and lead(II) ions was probed with luminescence spectroscopy, showing the interrelation between $[Au(CN)_2]^-$ anions and the lead(II) center. In another relevant example, in a series of $Zn[Au(CN)_2]_2$ polymorphs, each was shown to have a unique emission energy that correlated with the Au···Au distances; all polymorphs showed vapoluminescent behavior with NH_3 gas.[29] The analogous Cu(II) system is vapochromic, but does not emit at room temperature (RT).[30]

With the goal of examining this fundamental difference in emission properties between the Cu(II) and the Zn(II) containing systems above, we turned to the $[M'(en)_2][M(CN)_2]_2$ (M = Ag, Au; M′ = Zn, Cu; en = ethylenediamine) series of isostructural compounds, in which the dicyanometallate building blocks adopt a perfectly linear one-dimensional (1D) polymeric chain in staggered configuration (Figure 1).[24,26,31,32] Polymeric gold chains show many interesting luminescence properties related to structural distortion (vapochromism and tribochromism) and electronic structure (multiple emissions).[33−35]

Table 1. Crystallographic Data for $[Zn(en)_2][Au(CN)_2]_2$

	$[Zn(en)_2][Au(CN)_2]_2$
empirical formula	$C_8H_{16}N_8Au_2Zn$
formula weight	683.58
crystal system	monoclinic
space group	$C2/m$
a, Å	10.4752(14)
b, Å	13.2072(18)
c, Å	6.3903(9)
β, deg	119.6460(10)
V, Å^3	768.36(18)
Z	2
T, K	200
λ, Å	0.71073
ρ_{calcd}, g cm^{-3}	2.954
μ, mm^{-1}	20.594
R^a ($I > 2.5\sigma(I)$)	0.0146
$R_w{}^a$ ($I > 2.5\sigma(I)$)	0.0159
goodness of fit	1.5157

[a] Function minimized $\sum w(|F_o| - |F_c|)^2$ where $w^{-1} = [\sigma^2(F_o)]$, $R = \sum||F_o| - |F_c||/\sum|F_o|$, $R_w = [\sum w(|F_o| - |F_c|)^2/\sum w|F_o|^2]^{1/2}$.

In this paper, we have explored the effects on photophysical properties of small distortions in the $[M(CN)_2]_n$ linear chain chromophore and of the change in electronic properties due to the neighboring closed shell Zn(II) d^{10} ion or an open shell Cu(II) d^9 metal center. We report for the first time the effects of closed shell Zn(II) ions and Cu(II) open shell ions on the electronic properties of $Au(CN)_2^-$ polymeric compounds.

Experimental Section

Sample Preparation and Characterization. All materials were obtained from commercial sources and used as received. The coordination polymers $[M(en)_2][Au(CN)_2]_2$ (M = Cu[24] or Zn[26]) and $[M(en)_2][Ag(CN)_2]_2$ (M = Cu[31,32] or Zn[32]) were prepared as previously described. Crystalline materials were characterized by infrared (Supporting Information), luminescence, and UV−visible spectroscopy (vide infra). The IR spectra of all compounds exhibit characteristic C≡N stretching modes between 2137 cm^{-1} and 2152 cm^{-1}.

Spectroscopy. Reflectance spectra were recorded by an Ocean Optics usb4000 spectrometer coupled to a fiber optic probe. Halogen and helium arc lamps were used as light sources. Infrared spectroscopy was carried out with a Spectrum One FT-IR spectrometer (Perkin-Elmer Instruments) coupled to an ATR sampling accessory from Pike Technologies.

Steady-state photoluminescence spectra of the crystalline samples were recorded with a Model QuantaMaster-1046 photoluminescence spectrophotometer from Photon Technology International. The instrument is equipped with two excitation monochromators and a single emission monochromator with a 75 W xenon lamp. Low temperature steady-state photoluminescence measurements were achieved by using a Janis ST-100 optical cryostat equipped with a Honeywell temperature controller. Liquid nitrogen or liquid helium were used as coolants.

(23) Colis, J. C. F.; Larochelle, C.; Staples, R.; Herbst-Irmer, R.; Patterson, H. H. *Dalton Trans.* **2005**, *4*, 675–679.
(24) Leznoff, D. B.; Xue, B.; Batchelor, R. J.; Einstein, F. W. B.; Patrick, B. O. *Inorg. Chem.* **2001**, *40*, 6026–6034.
(25) Leznoff, D. B.; Xue, B.; Patrick, B. O.; Sanchez, V.; Thompson, R. C. *J. Chem. Soc., Chem. Commun.* **2001**, 259–260.
(26) Aguiar, P. M.; Katz, M. J.; Leznoff, D. B.; Kroeker, S. *Phys. Chem. Chem. Phys.* **2009**, *11*, 6925–6934.
(27) Černák, J.; Orendáč, M.; Potočňák, I.; Chomič, J.; Orendáčová, A.; Skoršepa, J.; Feher, A. *Coord. Chem. Rev.* **2002**, *224*, 51–66.
(28) Katz, M. J.; Michaelis, V. K.; Aguiar, P. M.; Yson, R.; Lu, H.; Kaluarachchi, H.; Batchelor, R. J.; Schreckenbach, G.; Kroeker, S.; Patterson, H. H.; Leznoff, D. B. *Inorg. Chem.* **2008**, *47*, 6353–6363.
(29) Katz, M. J.; Ramnial, T.; Yu, H. Z.; Leznoff, D. B. *J. Am. Chem. Soc.* **2008**, *130*, 10662–10673.
(30) Lefebvre, J.; Batchelor, R. J.; Leznoff, D. B. *J. Am. Chem. Soc.* **2004**, *126*, 16117–16125.
(31) Černák, J.; Chomič, J.; Gravereau, P.; Orendáčová, A.; Orendáč, M.; Kováč, J.; Feher, A.; Kappenstein, C. *Inorg. Chim. Acta* **1998**, *281*, 134–140.
(32) Kappenstein, C.; Ouali, A.; Guerin, M.; Černák, J.; Chomič, J. *Inorg. Chim. Acta* **1988**, *147*, 189–197.
(33) Yam, V. W. W.; Cheng, E. C. C. *Top. Curr. Chem.* **2007**, *281*, 269–309.
(34) Balch, L. *Struct. Bonding (Berlin)* **2007**, *123*, 1–40.
(35) Lopez-de-Luzuriaga, J. M. In *Modern Supramolecular Gold Chemistry: Gold-Metal Interactions and Applications*; Laguna, A., Ed.; John Wiley & Sons: Sussex, U.K., 2008; p 347.
(36) Frisch, M. J.; Trucks, G. W.; Schlegel, H. B.; Scuseria, G. E.; Robb, M. A.; Cheeseman, J. R.; Zakrewski Jr. V. G.; Montgomery, J. A.; Stratmann, R. E.; Burant, J. C.; Dapprich, S.; Millam, J. M.; Daniels, A. D.; Kudin, K. N.; Strain, M. C.; Farkas, O.; Tomasi, J.; Barone, V.; Cossi, M.; Cammi, R.; Mennucci, B.; Pomelli, C.; Adamo, C.; Clifford, S.; Ochterski, J.; Petersson, G. A.; Ayala, P. Y.; Cui, Q.; Morokuma, K.; Malick, D. K.; Rabuck, A. D.; Raghavachari, K.; Foresman, J. B.; Cioslowski, J.; Ortiz, J. V.; Baboul, A. G.; Stefanov, B. B.; Liu, G.; Liashenko, A.; Piskorz, P.; Komaromi, I.; Gomperts, R.; Martin, R. L.; Fox, D. J.; Keith, T.; Al-Laham, M. A.; Peng, C. Y.; Nanayakkara, A.; Challacombe, M.; Gill, P. M. W.; Johnson, B.; Chen, W.; Wong, M. W.; Andres, J. L.; Gozalez, C.; Head-Gordon, M.; Replogle, E. S.; Pople, J. A. *Gaussian'03*, Revision C.02; Gaussian,Inc.: Wallingford, CT, 2003.

Table 2. Selected Bond Lengths (Å) and Angles (deg) for $[Zn(en)_2][Au(CN)_2]_2$ at 200 K[a]

Zn(1)−N(1)	2.323(4)	Zn(1)−N(1)″	2.323(4)
Zn(1)−N(11)	2.126(3)	Zn(1)−N(11)*	2.126(3)
Zn(1)−N(11)′	2.126(3)	Zn(1)−N(11)″	2.126(3)
Au(1)−Au(2)	3.1951(4)	Au(1)−Au(2)†	3.1951(4)
N(1)−Zn(1)−N(11)′	90.80(10)	N(1)−Zn(1)−N(11)*	89.20(10)
N(1)−Zn(1)−N(11)″	90.80(10)	N(1)−Zn(1)−N(11)″	89.20(10)
N(1)″−Zn(1)−N(11)	89.20(10)	N(1)″−Zn(1)−N(11)*	90.80(10)
N(1)″−Zn(1)−N(11)′	89.20(10)	N(1)″−Zn(1)−N(11)″	90.80(10)
N(1)−Zn(1)−N(1)″	180	N(11)−Zn(1)−N(11)*	82.18(15)
N(11)−Zn(1)−N(11)′	97.82(15)	N(11)−Zn(1)−N(11)″	180
N(11)*−Zn(1)−N(11)′	180	N(11)*−Zn(1)−N(11)″	97.82(15)
N(11)′−Zn(1)−N(11)″	82.18(15)	Zn(1)−N(11)−C(11)	107.1(2)

[a] Symmetry transformations: * = 3−*x*, *y*, −*z*; ′ = *x*, 1−*y*, *z*; ″ = 3−*x*, 1−*y*, −*z*; † = *x*, *y*, −1+*z*.

Computational Details. Theoretical calculations on the $\{[Zn(en)_2]_2[Au(CN)_2]_3\}^-$ crystallographic substructure (C_{2h} symmetry) were done using the Gaussian '03 software (Gaussian Inc.).[36] Density functional theory (DFT) single point calculations were performed using the B3LYP functional[37−39] and SDD basis sets[40,41] as implemented by the software. The time-dependent theory (TD-DFT)[42−44] was used to calculate excited state energies. Molecular isodensity diagrams (Isovalue = 0.02 atomic units) of molecular orbitals were created by the GaussView 3.0 software (Gaussian Inc.).

Single Crystal X-ray Crystallographic Analysis. Crystallographic data for $[Zn(en)_2][Au(CN)_2]_2$ at 200 K is given in Table 1. A colorless crystal of $[Zn(en)_2][Au(CN)_2]_2$ having dimensions $0.40 \times 0.15 \times 0.07$ mm^3 was glued onto a glass fiber. The crystal was cooled to 200 K using an Oxford Cryosystems Cryostream system. The data range $4.4° \leq 2\theta \leq 56.7°$ was acquired on a Bruker SMART APEX-II diffractometer with graphite monochromated Mo Kα radiation (λ = 0.71073 nm), with a crystal-to-detector distance of 60 mm. The data was processed and corrected for Lorentz and polarization effects and an empirical absorption correction was applied.

The structure was solved via direct methods (SIR 92) with subsequent least-squares refinements in CRYSTALS.[45] The coordinates and anisotropic displacement parameters for the non-hydrogen atoms of $[Zn(en)_2][Au(CN)_2]_2$ were refined. Hydrogen atoms were placed in geometrically calculated positions, and refined using a riding model, and a constrained isotropic thermal parameter. The final refinement using observed data ($I_o \geq 2.50\sigma(I_o)$) and statistical weights included 55 parameters for 805 unique reflections. Selected bond lengths and angles are given in Table 2.

Results and Discussion

Structure of $[Cu/Zn(en)_2][M(CN)_2]_2$. The structures of the $[Cu(en)_2][M(CN)_2]_2$ (M = Au;[24] Ag[31]) and $[Zn(en)_2][M(CN)_2]_2$ (M = Au;[26] Ag[32]) materials have been previously reported and are essentially isostructural. However, the previously reported Zn/Au-containing structure was determined at RT,[26] while the Cu(II)-analogue was determined at 198 K.[24] To be able to make a clear comparison between structural features (particularly Au−Au bond distances) and their impact on the emission properties, the crystal structure of $[Zn(en)_2][Au(CN)_2]_2$ was redetermined at 200 K and the results are included herein. In all cases, the structures contain two inequivalent $[M(CN)_2]^-$ units, each of which has a linear, two-coordinate metal center.[24,26,31,32] The $[M(CN)_2]^-$ moieties aggregate in a staggered arrangement into 1D chains via M−M interactions. The aurophilic interactions are slightly shorter (3.1405(2) and 3.1951(4) Å for Cu and Zn systems respectively) than their argentophilic analogues (3.1580(5) and 3.221(2) Å for Cu and Zn systems respectively) (Table 2).[24,31,32] The metallophilic 1D chains are cross-linked at every alternate $[M(CN)_2]$-unit by binding of both N-cyano donors to the axial positions of $[Cu/Zn(en)_2]^{2+}$ cations to yield 1D chains of $[(en)_2Cu/Zn\text{-}NCAuCN]^+$ units; the final result is a 2D sheet structure (Figure 2). The N-cyano bond distances to the Cu(II) centers are substantially longer (2.576(6) and 2.569(4) Å for M = Au and Ag respectively) than for the analogous Zn(II) analogues (2.323(3) and 2.305(4) Å for M = Au and Ag respectively),[24,31,32] reflecting the presence of the Jahn−Teller axis in the Cu(II) version.

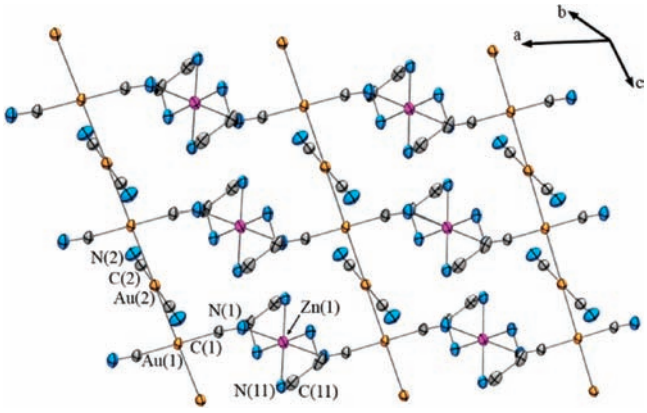

Figure 2. Representation of the 2D sheet structure of $[Zn(en)_2][Au(CN)_2]_2$. Independent atoms are labeled.

Diffuse Reflectance. Diffuse reflectance spectra of the different complexes are shown in Figure 3. Electronic absorption characterization was necessary to compare the excited state energies of emissive and non-emissive species (such as $[Cu(en)_2][Ag(CN)_2]_2$). In all compounds based on $[Cu(en)_2]^{2+}$ cations, a large absorption band (low %R) is seen at approximately 560 nm. In these materials, the copper ion is coordinated to 6 nitrogen atoms ($Cu(en)_2(NC)_2$). Diffuse reflectance spectra of compounds with a similar coordination sphere show a strong d-d transition at ~555 nm.[46] In these copper(II) complexes, the low energy, broad absorption transition is therefore assigned to the d-d absorption of the d^9 metallic center. Stronger absorption bands are seen at higher energy for all compounds. In dicyanoaurate and -argentate polymers, strong MLCT (d→π*) transitions are expected in this spectral region.[23]

(37) Becke, D. *J. Chem. Phys.* **1993**, *98*, 5648–5652.
(38) Lee, C.; Yang, W.; Parr, R. G. *Phys. Rev.* **1988**, *B37*, 785–789.
(39) Miehlich, B.; Savin, A.; Stoll, H.; Preuss, H. *Chem. Phys. Lett.* **1989**, *157*, 200–206.
(40) Dunning, T. H., Jr.; Hay, P. J.; Schaefer, H. F., III *Modern Theoretical Chemistry*; Plenum: New York, 1976; Vol. *3*.
(41) Fuentealba, P.; Preuss, H.; Stoll, H.; Von Szentpaly, L. *Chem. Phys. Lett.* **1982**, *89*, 418–422.
(42) Stratmann, R. E.; Scuseria, G. E.; Frisch, M. J. *J. Chem. Phys.* **1998**, *109*, 8218–8224.
(43) Bauernschmitt, R.; Ahlrichs, R. *Chem. Phys. Lett.* **1996**, *256*, 454–464.
(44) Casida, M. E.; Christine, J.; Casida, K. C.; Salahub, D. R. *J. Chem. Phys.* **1998**, *108*, 4439–4449.
(45) Betteridge, P. W.; Carruthers, J. R.; Cooper, R. I.; Prout, K.; Watkin, D. J. *J. Appl. Crystallorg.* **2003**, *36*, 1487.
(46) Akitsu, T.; Einaga, Y. *Inorg. Chim. Acta* **2008**, *361*, 36–42.

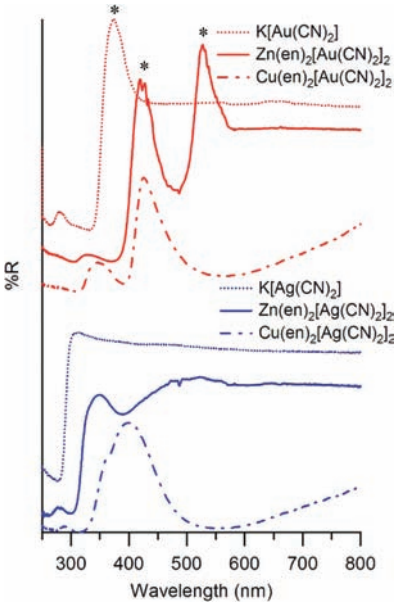

Figure 3. RT reflectance spectra of $K[M(CN)_2]$ and $[M'(en)_2][M(CN)_2]_2$ (M = Au, Ag and M′ = Zn, Cu) complexes. Peaks arising from a luminescence phenomenon are marked with an asterisk.

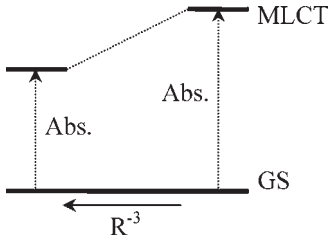

Figure 4. Inter-monomer dependency of the MLCT transition energy.

The energy and the number of observed electronic transitions in the UV−vis region should be directly related to the strength of the metallophilic interactions. As the metal−metal separation becomes smaller, it is expected that the strength of the metallophilic interactions increases. X-ray diffraction showed that at 200 K, the Au−Au distance in $[Cu(en)_2][Au(CN)_2]_2$ is 3.1405(2) Å and 3.1951(4) Å in the zinc analogue. This is observed in the reflectance spectra, where the $[Cu(en)_2][Au(CN)_2]_2$ absorbs at 392 nm (25 500 cm^{-1}) and $[Zn(en)_2][Au(CN)_2]_2$ absorbs at 370 nm (27 000 cm^{-1}). These absorption bands (low %R) are at lower energy than the corresponding $K[Au(CN)_2]$ absorption band observed at 330 nm (30 300 cm^{-1}). In the latter compound, the shortest Au−Au (at RT) is 3.64 Å.[23] As shown in Figure 4, a temperature study on $K[Au(CN)_2]$ showed that the MLCT emission band follows a Frenkel exciton behavior, where the energy is proportional to $-k(d_{Au-Au})^{-3}$.[23] At RT, the larger metal−metal distance seen in $K[Au(CN)_2]$ explains the observed high energy absorption band.

A small absorption band at 479 nm (20 900 cm^{-1}) is seen for the $[Zn(en)_2][Au(CN)_2]_2$, but no such low energy band is seen in the copper analogue. Excitation at this energy leads to emission (vide infra). We assume that a similar band should be observed in both the Zn and the Cu-dicyanoaurate compounds because they are isostructural, but the d-d transition present in the copper analogue shrouds this spectral region. In $[Zn(en)_2][Au(CN)_2]_2$, this band is bordered by two artifact peaks (%R > baseline) corresponding to RT luminescence, which can slightly affect the observed intensity and λ_{max}. Nonetheless, because of its spectral region and luminescence experiments, this band is assigned to another MLCT transition. Absorption band assignments and energies are given in Table 3.

Table 3. Wavelengths and Assignments for the Characteristic Absorption Bands for $[M'(en)_2][M(CN)_2]_2$ (M = Ag, Au and M′ = Cu, Zn) Compounds and $K[M(CN)_2]$

compound	λ_{max} (nm)	ν (cm^{-1})	assignments
$[Cu(en)_2][Au(CN)_2]_2$	310	32 300	MLCT $[Au(CN)_2]^-$
	392	25 500	MLCT $[Au(CN)_2]^-$
	564	17 700	d-d $[Cu(en)_2]^{2+}$
$[Zn(en)_2][Au(CN)_2]_2$	304	32 900	MLCT $[Au(CN)_2]^-$
	370	27 000	MLCT $[Au(CN)_2]^-$
	479	20 900	MLCT $[Au(CN)_2]^-$
$K[Au(CN)_2]$	330	30 300	MLCT $[Au(CN)_2]^-$
$[Cu(en)_2][Ag(CN)_2]_2$	313	32 000	MLCT $[Ag(CN)_2]^-$
	559	17 900	d-d $[Cu(en)_2]^{2+}$
$[Zn(en)_2][Ag(CN)_2]_2$	299	33 400	MLCT $[Ag(CN)_2]^-$
	390	25 600	MLCT $[Ag(CN)_2]^-$
$K[Ag(CN)_2]$	280	35 700	MLCT $[Ag(CN)_2]^-$

In comparison to the gold-materials, the silver-containing compound exhibits characteristic MLCT bands at higher energy than the gold cases. Such metal-dependent behavior is also seen for the pure potassium dicyanometallate salts. Similar to the gold-based compounds, the $[Zn(en)_2][Ag(CN)_2]_2$ absorbs at generally higher energy than its copper analogue. Furthermore, a weaker band is seen at low energy (390 nm, 25 600 cm^{-1}) in the zinc analogue. This absorption band corresponds to an excitation peak observed by emission spectroscopy (vide infra) and is therefore assigned to a dicyanoargentate-based MLCT transition.

Luminescence. In the title compounds, a 1D polymeric $\{[M(CN)_2]^-\}_n$ chain is present and MLCT luminescence energy is expected to vary with the metallophilic interaction strength. Chains are cross-linked by $[M'(en)_2]^{2+}$ (M′ = Zn or Cu) cations. Careful selection of this metallic linker allows for tunability of the photophysical properties of the material. While a closed-shell d^{10} zinc center is relatively inactive, an open-shell d^9 copper center offers new deactivation pathways via energy transfer in its d-d excited states or via a low energy electron transfer state (MMCT). Reflectance spectra of our compounds exhibit d-d transitions but no metal-to-metal charge transfer band. Energy transfer was therefore considered to be the predominant deactivation phenomenon. Luminescence spectra are shown in Figures 5 and 6 while spectroscopic results are summarized in Table 4.

The first noticeable feature of these spectra is the multiple emissions observed for the emissive compounds. This phenomenon was already seen in other gold 1D polymeric chains,[47] and the emissions were assigned to spin-allowed and spin-forbidden transitions of different types (Ligand to Metal Charge Transfer versus Metal Centered). As previously mentioned, in d^{10} metal dicyano compounds, the ligand centered π^* orbital mixes with the metal centered p orbitals and a fast internal conversion is expected between the high energy MC excited state and

(47) Lee, Y.-A.; McGarrah, J. E.; Lachicotte, R. J.; Eisenberg, R. *J. Am. Chem. Soc.* **2002**, *124*, 10662–10663.

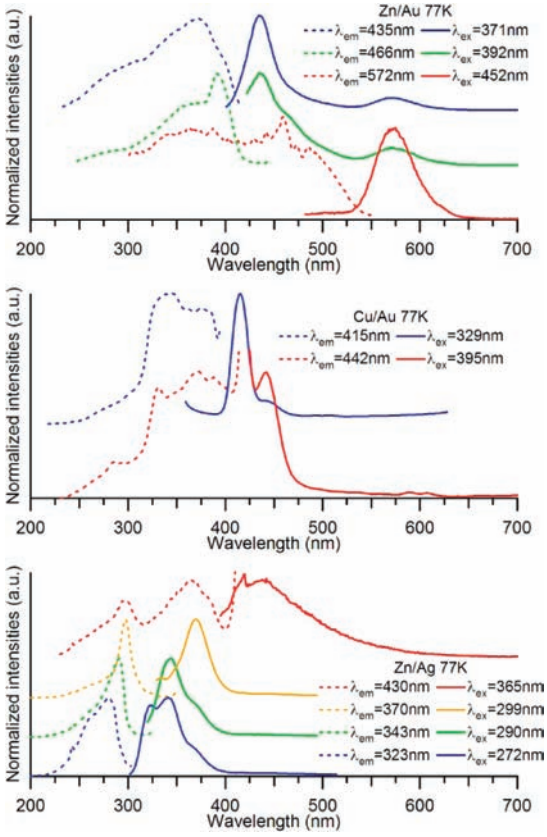

Figure 5. Luminescence spectra of $[M'(en)_2][M(CN)_2]_2$ (M = Ag, Au; M′ = Zn, Cu) complexes at 77 K (spectra at other temperatures are included in the Supporting Information).

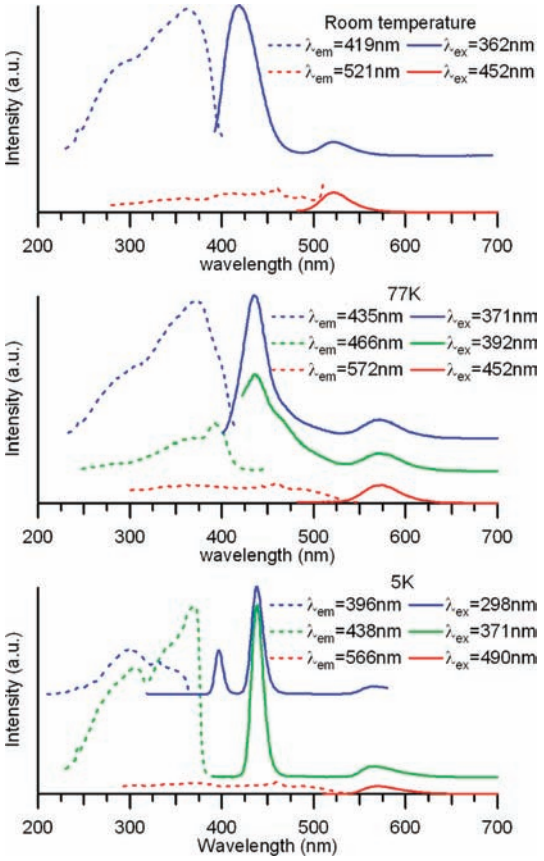

Figure 6. Luminescence spectra of $[Zn(en)_2][Au(CN)_2]_2$ at RT, 77 K and 5 K.

the lower energy MLCT state. Therefore, no emission from a pure MC state is expected to be seen in these compounds. We propose that these multiple peaks correspond to MLCT transitions between the gold or silver d orbital and different π*-orbitals of the cyanides.

A comparison between the copper and zinc analogues shows another interesting trend. The $[Cu(en)_2][Ag(CN)_2]_2$ is non-emissive at any temperature, and no emission is seen at RT for the $[Cu(en)_2][Au(CN)_2]_2$ while the zinc compounds exhibit relatively strong emission at any temperature. Moreover, in the copper compounds, no low energy emission peak (λ_{em} = ~520−560 nm) is seen at any temperature. These spectral characteristics can be connected to the presence of low energy d−d excited states in the d^9 Cu(II) ions. In $[Zn(en)_2][Au(CN)_2]_2$, the strong emission bands red-shift when the temperature is reduced. This phenomenon is related to the Au−Au distance contraction at lower temperature; the Au−Au distance in $Zn(en)_2[Au(CN)_2]_2$ changes from 3.2201(6) Å at 300 K[26] to 3.1951(4) Å at 200 K. This trend has also been observed in variable-temperature crystallographic studies of $[Au(CN)_2]^-$ based coordination polymers such as $KAu(CN)_2$[48] and $KCd[Au(CN)_2]_3$[49] and is consistent with the MLCT nature of the emission bands.

Ab Initio Calculations. DFT calculations were carried out on $\{[Zn(en)_2(NH_3)]_2[M(CN)_2]_1\}^{+3}$ and $\{[Zn(en)_2(NH_3)]_2[M(CN)_2]_3\}^{+1}$ (M = Ag or Au) complexes. The positions of hydrogen and nitrogen (NH_3) atoms were optimized while other atomic positions were taken from the crystallographic structures of $[Zn(en)_2][Ag(CN)_2]_2$[32] or $[Cu(en)_2][Ag(CN)_2]_2$[31] at RT, and $[Zn(en)_2][Au(CN)_2]_2$[26] or $[Cu(en)_2][Au(CN)_2]_2$[24] at 200 K. To complete the coordination

Table 4. Characteristic Excitation and Emission Wavelength of MLCT Band Maxima for $[M'(en)_2][M(CN)_2]_2$ (M = Ag, Au and M′ = Zn, Cu) Compounds[a]

sample	*T* (K)	$\lambda_{max\ ex}$ (nm)	$\lambda_{max\ em}$ (nm)
$[Zn(en)_2][Au(CN)_2]_2$	RT	361	418
		~460	522
	77	372	436
		391*w*	466*w*
		~470	568
	5	300, 350	396
		370	437
		~470	566
$[Cu(en)_2][Au(CN)_2]_2$	RT	no emission	
	77	330−385*b*	415
		330−400*b*	442
	5	325−375*b*	411
		330−370*b*, 402	439
$[Zn(en)_2][Ag(CN)_2]_2$	RT	302	350
		366	434
	77	280	322
		291	344
		298	370
		365	438
	5	290	343
		296	370
		366	436
$[Cu(en)_2][Ag(CN)_2]_2$	RT, 77, 5	no emission	

[a] *b* and *w* stands for broad and weak respectively.

(48) Nagasundaram, N.; Roper, G.; Biscoe, J.; Chai, J. W.; Patterson, H. H.; Blom, N.; Ludi, A. *Inorg. Chem.* **1986**, *25*, 2947–2951.
(49) Korcok, J. L.; Katz, M. J.; Leznoff, D. B. *J. Am. Chem. Soc.* **2009**, *131*, 4866–4871.

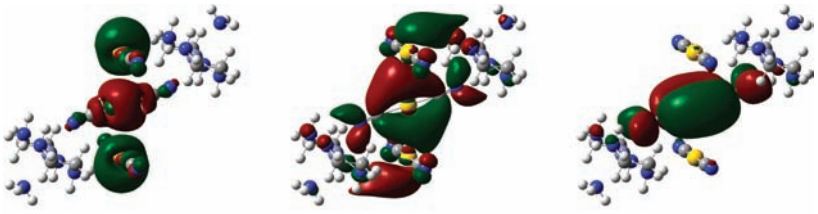

Figure 7. Isodensity diagrams of HOMO d_{z^2}(Au), LUMO p(Au)/π*(CN) and of a higher energy non-bonding p(Au)/π*(CN) orbitals of the $\{[Zn(en)_2(NH_3)]_2[Au(CN)_2]_3\}^{+1}$ complex.

Table 5. Theoretical Transition Energies for $\{[Zn(en)_2(NH_3)]_2[M(CN)_2]_1\}^{+3}$ and $\{[Zn(en)_2(NH_3)]_2[M(CN)_2]_3\}^{+1}$ (M = Ag or Au) Species with Structural Features of the Corresponding X-ray Diffraction Structure[24,25,31,32]

			λ_{MLCT} (nm)	
complexes	X-ray structure	d_{M-M} (Å)	$^1\Gamma \rightarrow {}^3\Gamma$	$^1\Gamma \rightarrow {}^1\Gamma^a$
$\{[Zn(en)_2(NH_3)]_2[Au(CN)_2]_1\}^{+3}$	$[Cu(en)_2][Au(CN)_2]_2$		240.3	215.2 (0.0744)
	$[Zn(en)_2][Au(CN)_2]_2$		237.1	211.9 (0.0636)
$\{[Zn(en)_2(NH_3)]_2[Au(CN)_2]_3\}^{+1}$	$[Cu(en)_2][Au(CN)_2]_2$	3.1405	331.8	299.4 (0.3805)
	$[Zn(en)_2][Au(CN)_2]_2$	3.1951	327.3	294.2 (0.4085)
$\{[Zn(en)_2(NH_3)]_2[Ag(CN)_2]_1\}^{+3}$	$[Cu(en)_2][Ag(CN)_2]_2$		232.7	209.4 (0.0909)
	$[Zn(en)_2][Ag(CN)_2]_2$		234.4	213.7 (0.0712)
$\{[Zn(en)_2(NH_3)]_2[Ag(CN)_2]_3\}^{+1}$	$[Cu(en)_2][Ag(CN)_2]_2$	3.158	307.8	286.8 (0.2814)
	$[Zn(en)_2][Ag(CN)_2]_2$	3.221	296.6	275.4 (0.3117)

[a] Oscillator strengths for the spin-allowed transitions are in parentheses.

sphere of the zinc or copper ions, optimized ammine ligands were added instead of crystallographic N-coordinated cyanide anions. Isodensity contour maps of some orbitals responsible for allowed MLCT transitions are shown in Figure 7.

d^{10} cyanometallate ions are known to exhibit strong luminescence arising from a MLCT transition.[17,18,23] In these linear compounds, the highest occupied molecular orbital (HOMO) orbital consists of the d_{z^2} metal orbital while the cyanide π* orbital mixes with an empty metal p orbital to form the lowest unoccupied molecular orbital (LUMO). In compounds where metallophilic interactions are observed, the energy of the electronic transition decreases because of the metal character portion of both the HOMO and the LUMO. When two metals centers are close, the d_{z^2} orbitals interact in an anti-bonding fashion, increasing the energy of the dimer HOMO. Similarly, the π*/p orbitals interact in a bonding fashion, when the metal p orbitals are aligned with the M−M axis. Other orientations may yield higher energy π*/p molecular orbitals.

The HOMO corresponds to the d_{z^2} metal orbital of the dicyanometallate ions and exhibits anti-bonding character with the cyanide ligands and between the metal centers. The lowest empty π*(CN) orbital shows delocalization with a p orbital of the d^{10} metal centers and minimal delocalization into the $[M(en)_2(NH_3)]^{2+}$ units. For $\{[Zn(en)_2(NH_3)]_2[M(CN)_2]_3\}^{+1}$ (M = Ag or Au), the empty metal p orbitals interact in a bonding fashion along the M_3 chain. It should be noted that four different π*(CN) orbitals with different orientations and symmetry are expected for every $[M(CN)_2]^-$ unit. Furthermore, two singularly different dicyanometallate units are present in these complexes. One is capped by two zinc or copper centers while the second is not interacting with the $[M(en)_2]^{2+}$ units. Also, when π*/p orbitals are aligned along the M−M axis, they interact in a bonding or anti-bonding fashion, while orbitals oriented perpendicularly to this axis do not interact with one another and are considered to have a M−M non-bonding character. After a MLCT transition, the nature of these π*(CN) orbitals dictates intensity and direction of the structural variation between the ground and the excited states. In the lowest energy MLCT excited states, the CN bond elongates while the M−C distance shortens, as does the M−M distance. Because of this stronger metal−metal interaction in the excited state, dicyanometallate anions exhibit excimeric behavior.[17−20,50,51]

The studied monomeric and trimeric species do not perfectly represent the 1D polymeric $\{[M(CN)_2]^-\}_n$ chain seen in the crystallographic structure. An increase in the number of interacting metallophilic units should result in a lowering of the bonding π*(CN)/p(M) orbital's energy and an increase of the anti-bonding d_{z^2}(M) orbital's energy, with a net decrease of the energy gap between these two and therefore a lowering of the corresponding transition energy. This can be seen in Table 5, where transition energies found by TD-DFT are reported for monomeric and trimeric species. In general, increasing the nuclearity of the $[M(CN)_2]^-$ chain from 1 to 3 decreases the absorption MLCT transition energy by a factor of 11300 cm^{-1} for the gold compounds and 9700 cm^{-1} for the silver analogues. The lowest energy excitation found for $[Zn(en)_2][Au(CN)_2]_2$ is at ~470 nm (21250 cm^{-1}) which is approximately 10000 cm^{-1} lower in energy than is the 327.3 nm (30553 cm^{-1}) calculated for the trimeric species. This further red-shift is due to the polymeric nature of the $\{[Au(CN)_2]^-\}_n$ chain in the pure compound. Similar offset between experimental and theoretical energies was seen for all the compounds.

Another interesting feature of the TD-DFT calculations is the small energy difference between models based

(50) Patterson, H. H.; Kanan, S. M.; Omary, M. A. *Coord. Chem. Rev.* **2000**, *208*, 227–241.
(51) Rawashdeh-Omary, M. A.; Omary, M. A.; Shankle, G. E.; Patterson, H. H. *J. Phys. Chem. B* **2000**, *104*, 6143–6151.

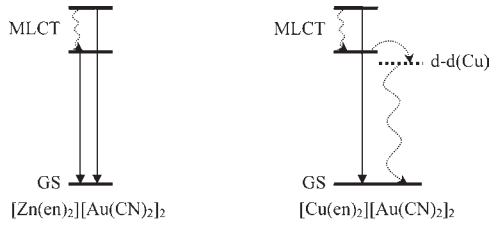

Figure 8. Electronic state diagram of $[Zn(en)_2][Au(CN)_2]_2$ and $[Cu(en)_2][Au(CN)_2]_2$. Emissions are represented by downward arrows while deactivation pathways are represented by dashed arrows.

on the Cu(II) versus Zn(II) materials. In dicyanoaurate complexes, the theoretical HOMO−LUMO transition energy of the copper compounds is systematically smaller ($\sim$1000 cm^{-1}). This is in agreement with reflectance experiments where corresponding MLCT absorption bands are 600 and 1500 cm^{-1} lower in energy for the copper compound. This can be correlated to the Au−Au distance (3.1405(2) Å in $[Cu(en)_2][Au(CN)_2]_2$ and 3.1915(4) Å in $[Zn(en)_2][Au(CN)_2]_2$). A similar behavior is observed for the dicyanoargentate complexes. The shorter distance promotes an orbital energy shift due to the bonding or anti-bonding character along the M−M interaction. In this case, the d_{z^2}(M) increases in energy while the π^*(CN)/p(M) energy decreases, yielding in a global reduction of the HOMO−LUMO transition energy.

The lower energy emission of $[Zn(en)_2][Au(CN)_2]_2$ is not seen for the isostructural $[Cu(en)_2][Au(CN)_2]_2$. For closely related complexes such as these two compounds, similar excitation and emission peaks should be observed. In a copper compound, the presence of Cu(II) ions yields extra excited states than with the Zn(II) ion case. However, in $[Cu(en)_2][Au(CN)_2]_2$, the non-emissive copper(II) centered d-d band overlaps with the expected low energy $\{[Au(CN)_2]^-\}_n$ centered emission ($\sim$520−560 nm in the zinc complex). We believe that energy transfer occurs between the two chromophores followed by a rapid non-radiative decay to the ground state. Compared to higher energy MLCT states, this enhanced deactivation process is much more efficient for the lower energy HOMO−LUMO state and may explain the missing emission band in the $[Cu(en)_2][Au(CN)_2]_2$ luminescence spectra as well as the total lack of emission for $[Cu(en)_2][Ag(CN)_2]_2$. These observations allow us to propose an electronic state diagram, shown in Figure 8.

While this anti-bonding d_{z^2}(M) → bonding π^*(CN)/p(M) assignment explains the low energy transition observed, it cannot explain the higher energy excitation and absorption observed (330−400 nm). As described earlier, π^*(CN) is a family of orbitals with different orientation and energy. Transitions from the anti-bonding d_{z^2}(M) to non-bonding or even anti-bonding π^*(CN) would yield a higher energy excitation/emission, consistent with what is observed here. The difference in interaction character gives structurally and energetically different excited states that can hinder deactivation to the lower energy state resulting in luminescence of these higher energy states.[28,52]

Conclusion

The $[M'(en)_2][M(CN)_2]_2$ (M′ = Zn, Cu; M = Ag, Au) complexes, which contain metallophilic 1D chains, showed interesting photophysical properties. Multiple absorption and emission bands were observed in compounds containing $\{[Au(CN)_2]^-\}_n$ infinite chains. We determined by DFT that these bands are transitions from anti-bonding d_{z^2}(Au) to π^*(CN) orbitals with different Au−Au bonding character. A low energy MLCT emission band was observed for the zinc analogue but not for the copper complex. We have proposed a mechanism in which copper(II) d-d excited states deactivate predominantly the low energy excited state through energy transfer.

Compared to the dicyanoaurate-based compounds, the analogues containing the $[Ag(CN)_2]^-$ building block show MLCT excited states at higher energy. The presence of the copper(II) d-d transition allows for a rapid and efficient deactivation of the MLCT states and therefore, no emission is observed for $[Cu(en)_2][Ag(CN)_2]_2$. Thus, in $[M'(en)_2][M(CN)_2]_2$ (M′ = Zn, Cu; M = Ag, Au) substitution at both metal sites allows for excited states energy tunability, as well as specific quenching of some emission bands.

Acknowledgment. This work was supported by the National Science Foundation (CHE-0315877). NSERC of Canada is gratefully acknowledged. We would like to acknowledge Professor Scott Collins (University of Maine) for his support with reflectance spectroscopy. We thank Mr. David LaBrecque for general assistance.

Supporting Information Available: A detailed infrared spectroscopy analysis and crystallographic data in CIF format for $[Zn(en)_2][Au(CN)_2]_2$. Additional emission spectra at RT are also included. This material is available free of charge via the Internet at http://pubs.acs.org.

(52) Assefa, Z.; DeStefano, F.; Garepapaghi, M. A.; LaCasce, J. H., Jr.; Ouellete, S.; Corson, M. R.; Nagle, J. K.; Patterson, H. H. *Inorg. Chem.* **1991**, *30*, 2868–2876.